

ARTICLE

Modeling Photo-dissociation Dynamics of HBr^+ by Vibrational Wave-packet Formalism

Chandan Kumar Mondal*, Bikram Nath

Department of Chemistry, Physical Chemistry Section, Jadavpur University, Kolkata 700032, India

(Dated: Received on January 21, 2012; Accepted on April 11, 2012)

Photo dissociation dynamics of diatomic molecular ion HBr^+ interacting with ultra fast laser pulses of different envelop function has been presented both in zero and non zero temperature environment. The calculations pertain primarily to the ground electronic state of the molecular ion HBr^+ . The used potential of HBr^+ is calibrated with the help of the *ab initio* theoretical calculation at the CCSD/6-311++G(3df, 2pd) level and then fitted with appropriate Morse parameters. The numerical bound states vibrational eigenvalues obtained by the time independent Fourier Grid Hamiltonian method have been compared with analytical values of the fitted Morse potential. The effect of temperature, pulse envelops function, and light intensity on the dissociation process has been explored.

Key words: Photo-dissociation, Thermal effect, Fourier Grid Hamiltonian method, Pulse envelop function, Bichromatic field

I. INTRODUCTION

If a molecule or molecular ion system is placed in a steady electromagnetic field, the coulomb binding forces of the molecule are supplemented by an additional force which tends to separate the charges. One would expect that a sufficiently intense electromagnetic field would lead to a dissociation of the system. The quantum dynamics of a periodically forced Morse oscillator is inherently interesting as it helps us to understand the photo-dissociation dynamics of a real diatomic molecule [1, 2]. The rich interactions between intense ultra short laser pulses and molecules have driven a large amount of researcher [3–9], since it can increase our level of understanding about laser-matter interactions. Quantum simulations of such interactions at the highest available level of accuracy are an important complement to experimental work [10–12]. However, the ability to simulate strong field interactions using a variety of more approximate methods can lead to a deeper understanding of the underlying chemistry and physics. The study of photo-detachment in the gas phase in presence of electric field has proved to be immensely important in sharpening our understanding in the field of spectroscopy of radicals, transition states and intermediates of chemical reactions. The study of photo-detachment on atomic anion in the solution phase [13, 14] may also increase our basic understanding about laser matter interaction. Both classical [15, 16] and quantum mechanical [16–18]

methods agree that high intensities are needed for dissociation due to the small vibrational transition moment. These intensities are relatively higher for the strongly bound diatomic molecular ion systems than the diatomic molecule. One important point which is generally neglected in the theoretical treatment is the rotation of the molecule. It is not clear until now that the rotation of the molecule would decrease the necessary intensities for the dissociation [19]. It had also been found that the dissociation probability was rather low when monochromatic sub-picoseconds pulse was used with low intensity [20]. The low efficiency had been traced to the mechanical anharmonicity of the vibrational potential which renders the monochromatic pulses ineffective for selective excitation. An appropriately chirped pulse was found to selectively excite the diatomic molecule to a higher vibrational state [21]. There is also an evidence of the existence of a critical intensity threshold and an induction period [22, 23] suggesting the existence of a bottle-neck problem [24] in the multi-photon dissociation of a diatomic molecule. If a diatomic molecule or molecular ion is not isolated or free but in an interacting environment, the situation is changed and the question of environmental perturbation influencing the photo-dissociation process needs to be addressed. Similarly, when the dissociation process occurs at non-zero temperatures [25, 26], and there is a distribution of population over vibrational levels to start with, there appears an additional factor that can affect the photo-dissociation rate.

In this work, to observe the thermal effects on the dissociation of a diatomic molecular ion in the presence of strong laser fields and the pulse shape effect on the dissociation process, we explore some quantum mechanical

*Author to whom correspondence should be addressed. E-mail: pcckm@yahoo.co.in, Tel.: +91-33-24572688, FAX: +91-33-24146223

ways to model the effects of environment and finite temperature on the dissociation process. The finite temperature effects are simulated by choosing an initial state that yields the thermal distribution of the population among different vibrational levels at the temperature concerned. As a system we have chosen the molecular ion HBr^+ , a molecular ion that has been the subject of both experimental and theoretical investigations. We have used the time dependent Fourier grid Hamiltonian (FGH) method [22, 27] in this exploration.

II. NUMERICAL METHOD AND COMPUTATIONAL DETAILS

For the computational and numerical procedure, we have used *ab initio* coupled-cluster singles and doubles (CCSD) method [28–30] with a UHF reference state function. Gaussian 03 [31] suit of programs was used for the *ab initio* molecular electronic structure calculations to calculate the total ground state energies of $\text{HBr}^+(X^2\Pi)$ against the inter nuclear distance. The *ab initio* calculations were performed using 6-311++G(3df, 2pd) basis set. We have frozen the ten core electrons of Br atom in the post HF calculations while all virtual molecular orbitals are included in the electron correlation that had been applied in the study of the excited states of BCl [32]. Although in some molecular systems, the excited states may affect the photo induced dissociation processes, however in the present molecular ion HBr^+ , the first excited state $A^2\Sigma^+$ is a bound state with a symmetry different from the ground state $X^2\Pi$ and has quite large transition energy of 320.8 meV from the ground state [33], so it may be assumed that the ground state potential energy surface (PES) is not affected by the higher excited state. It was also reported that the second excited state is a pure dissociating state and its PES does not cross the PES of the ground state because its dissociation limit is the same as that of the ground state [34]. For the numerical calculation, we start with the time dependent Schrödinger equation

$$i\hbar \frac{\partial |\Psi\rangle}{\partial t} = \hat{H} |\Psi\rangle \quad (1)$$

$$\begin{aligned} \hat{H} &= \frac{\hat{p}_x^2}{2m} + V_0(x) + V'(x, t) \\ &= \hat{H}_0 + V'(x, t) \end{aligned} \quad (2)$$

where $V_0(x)$ is the appropriately fitted Morse potential for the system and $V'(x, t)$ represents the dipole field interaction between the electric field of light and the molecular ion. We have used the FGH [35, 36] method to find out the ground state eigenfunctions and eigenvalues of \hat{H}_0 ,

$$\hat{H}_0 |\phi_i^0(x)\rangle = \varepsilon_i^0 |\phi_i^0(x)\rangle, \quad i = 1, 2, \dots, N \quad (3)$$

where N is the odd number [35] of equi-spaced grid points used for representing ϕ_i^0 in the coordinate grid

space of x values, $x_i = i\Delta x$. The basis bras and kets of our discretized coordinate space give the values of a wave function at the grid points. The identity operator is

$$\hat{I}_x = \sum_{i=1}^N |x_i\rangle \Delta x \langle x_i| \quad (4)$$

and the orthogonality condition now is written as $\Delta x \langle x_i | x_p \rangle \delta_{ip}$.

Following the recipe proposed by Marston and Balint-Kurti [35, 36], the renormalized Hamiltonian matrix elements are given as

$$\begin{aligned} \Delta x \langle x_i | \hat{H}_0 | x_p \rangle &= H_{ip}^0 \\ &= \frac{2}{N} \sum_{l=1}^n \left\{ \cos \left[\frac{2\pi l(i-p)}{N} \right] T_l + V_0(x_i) \delta_{ip} \right\} \end{aligned} \quad (5)$$

$$T_l = \frac{\hbar^2}{2m} \left(\frac{2\pi l}{N\Delta x} \right)^2 \quad (6)$$

where $2n = N + 1$. The FGH eigenfunctions computed by the recipe proposed by Marston and Balint-Kurti [35, 36] are

$$|\phi_i^0(x)\rangle = \sum_{p=1}^N |x_p\rangle \Delta x W_{ip}^0, \quad p = 1, 2, \dots, N \quad (7)$$

where W_{ip}^0 are the p th grid point amplitudes of the i th eigenstate of \hat{H}_0 . For the non-zero temperature situation ($T > 0$) [23–26], we assume that the different energy levels $\{\varepsilon_i^0\}$ of the unperturbed Morse oscillator are populated according to the Boltzmann distribution law:

$$n_i = n_i^0 \exp \left[\frac{-(\varepsilon_i - \varepsilon_0)}{kT} \right] \quad (8)$$

Consistently with the population distribution, the initial state $|\Psi(x, t = 0)\rangle$ may be described by the linear combination of the bound states of the approximately fitted Morse oscillator of the HBr^+ molecular ion system.

$$|\Psi(x, t = 0)\rangle = \sum_{i=1}^{n_b} A_i |\phi_i^0(x)\rangle \quad (9)$$

$$A_i = \pm \sqrt{\frac{n_i}{\sum n_i}} \quad (10)$$

where n_b is the total number of bound states, the phases of A_i may be randomly chosen. In this way we may incorporate the non-zero temperature effects in the simulated quantum dynamics.

For the time dependent problem, the eigenfunction $|\Psi(x, t)\rangle$ has been evolved under the action of \hat{H} which is represented as follows:

$$|\Psi(x, t)\rangle = \sum_{p=1}^N |x_p\rangle \Delta x W_p(t) \quad (11)$$

The representation is analogous to the Eq.(7) except that the grid point amplitudes are now time dependent quantities. If we now demand that $|\Psi(x, t)\rangle$ satisfies the Dirac-Frenkel time dependent variation principle, we arrive at the evolution equations for the grid point amplitudes:

$$\begin{aligned}\dot{W}_i &= \frac{1}{i\hbar} \sum_{p=1}^N [\langle x_i | H_0 | x_p \rangle + \langle x_i | V'(x, t) | x_p \rangle] W_p(t) \\ &= \frac{1}{i\hbar} \sum_{p=1}^N [H_{ip}^0 + V'(x_i, t)\delta_{ip}] W_p(t)\end{aligned}\quad (12)$$

It is the N coupled first order differential equation, which can be integrated by Runge-Kutta (4th order) method. To integrate Eq.(12) numerically we need the initial grid point amplitude of $W_i(t=0)$, which can be obtained straight forward from the Eqs.(7)–(9). We chose the Morse oscillator $V_0(x)$ and $V'(x, t)$ as the interacting Hamiltonian between the applied electromagnetic radiation and the target molecular ion.

$$V_0(x) = D_0 \{1 - \exp[-\beta(x - x_e)]\}^2 \quad (13)$$

$$x_e = \frac{h\nu}{4D_0} \quad (14)$$

$$\nu = \frac{\beta}{2\pi} \sqrt{\frac{2D_0}{\mu}} \quad (15)$$

$$V'(x, t) = \varepsilon_0 \mu(x) \sin(\omega t) S(t) \quad (16)$$

where D_0 and x_e represent the bond dissociation energy and the equilibrium bond length of the system, respectively [38]. ε_0 is the peak field intensity of the applied electrical field, $\mu(x)$ is the dipole moment operator and $S(t)$ is the pulse envelop function which is basically a slowly time varying function compared to the optical oscillation $\sin(\omega t)$. In our calculations we have taken three different forms: the sinusoidal function $S(t) = \sin^2(\pi t/t_p)$, Gaussian function $S(t) = e^{-\sigma(t-t_c)^2}$, and continuous function $S(t) = 1$.

The matrix elements appearing in the Eq.(11) can be evaluated by using the TDFGH [22, 25, 26] method. To calculate the dissociation probability, we have projected the evolving wave function on the time independent eigenfunction of H_0 which will produce the generalized overlap amplitude $s_i(t)$:

$$s_i(t) = \langle \Psi(x, t) | \phi_i^0(x, t=0) \rangle \quad (17)$$

If n_b is the number of bound states supported by H_0 , then the dissociation probability $P_d(t)$ at a particular instant of time t is given by

$$P_d(t) = 1 - \sum_{i=1}^{n_b} |s_i(t)|^2 \quad (18)$$

We have added absorbing complex potentials [37] to the Hamiltonian in order to avoid the non-physical reflections which are obtained due to the use of a finite grid

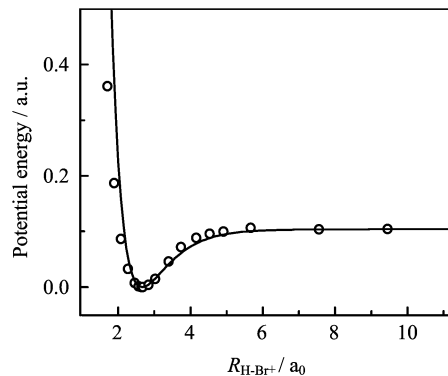


FIG. 1 Electronic ground state potential energy curve of HBr⁺ at CCSD level calculation using 6-311++G(3df, 2pd) as basis set and its appropriate fitted Morse potential.

in numerical calculations. By plotting $-\ln P_d(t)$ against time and computing the slopes at sharp rising point we have calculated the dissociation rate constant k_d . Now it is clear that k_d depends not only on ε_0 and ω but also on the temperature T and other parameters.

III. RESULTS AND DISCUSSION

In Fig.1, we show the ground state electronic potential of the system (HBr⁺) that was obtained using *ab initio* calculation at the CCSD/6-311++G(3df, 2pd) level and its fitted one in the appropriate Morse potential function (Eq.(13)). The fitted Morse parameters $D_0 = 0.104$ a.u. (272.79 kJ/mol), $\beta = 0.920$ a.u. (2.071 Å⁻¹), $x_e = 2.665$ a.u. (1.410 Å), $\mu = 1827.6322$ a.u. The dipole moment of the system as a function bond length have been calculated using the above mentioned *ab initio* method and was fitted in

$$\mu(x) = \mu_0 x \exp(-\sigma x^4) \quad (19)$$

where $\mu_0 = 190.5 \times 10^{-3}$ a.u. and $\sigma = 3.5 \times 10^{-3}$ a.u. The time-independent treatment of FGH method [35, 36] got the result that the number of bound states n_b for this system is 17. For the calculation we have taken 129 grid points and 0.075 a.u. of length as space step. We have placed the absorbing complex potential at the grid point of 45. The numerical energy eigenvalues for the bound states obtained by FGH method agree very well with the analytical solution of Morse potential, which is shown as follows, for different vibrational quantum states.

$$E_n = \left(n + \frac{1}{2}\right) h\nu - \chi_e \left(n + \frac{1}{2}\right)^2 h\nu \quad (20)$$

The good agreement of these two sets of energy eigenvalues makes us believe that the fitted parameters represent the Morse potential of HBr⁺ very well.

We have used three different types of pulse shape functions for the external field in our numerical calculations. First one is the continuous pulse, second

one is the sinusoidal with a period t_p and another is the Gaussian pulse. The value of t_p is connected with the pulse width, by (full wavelength at half maximum) $\text{FWHM}=0.364 t_p$. Generally, long pulse duration (large t_p) is necessary to study the dissociation process of diatomic molecules when the applied field intensity is weak, while short pulse duration (small t_p) is necessary for the strong electric field case. Our simulation time was 6×10^3 a.u. (145 fs) and time step was 0.03 a.u.. The pulse duration near 50 fs was found to be quite adequate to investigate the dissociation process for the field intensity range that has been used in the dynamical calculations. We have used a laser of frequency $\hbar\omega=0.02$ a.u. (4389 cm^{-1}) which is slightly off-resonant with the $0 \rightarrow 1$ vibrational transition frequency $\hbar\omega=11.04 \times 10^{-3}$ a.u. (2587 cm^{-1}) of the system. The choice of ε_0 is tricky. Since the HBr^+ is strongly bound, the reasonably strong peak field intensity should be applied to observe the dissociation. If the intensity is too strong, the dissociation of HBr^+ takes place immediately and it is impractical to study the dynamics. If the intensity is low, the rate of dissociation would also be too low and the time evolution has to be carried out over a long period of time which is also impractical in the current computational capacity. Therefore, we have used substantially high intensity of laser to make the problem practical. The maximum pulse duration has been simultaneously chosen in such a way that the laser induced tunnelling-ionization is not our concern over the time scale of the simulation.

When the electric field of light (slightly off resonance) is turned on, the molecular ion experiences excitation from the initial vibrational state, and the populations in the higher levels are seen to grow and decay systematically and sequentially. Generally, the survival probabilities for the higher vibrational levels initially start to increase, and after reaching the maximum they finally decrease to zero. But there are some minute differences for the excited states if we consider it in detail. For example, for the first excited state, the survival probability initially starts to increase, reaches a maximum, and decays systematically and sequentially. For the second excited state, the survival probability starts to increase a little later than that for the first excited state. Generally speaking, initially the total population at the ground vibrational level is equal to unit and that of the upper vibrational level is zero. At the beginning stage of the propagation the probabilities of the excited vibrational states increase, while that of the ground state decreases. When the survival probability of the higher level reaches maximum, the survival probability of the lower level is already in the monotonic decreasing behavior. There are more than one bound states supported by our system, and any excitation from the ground state contributes to the higher state population. The net growth of population in the unbound part of the spectrum represents the dissociation probability $P_d(t)$ which is the net probability of

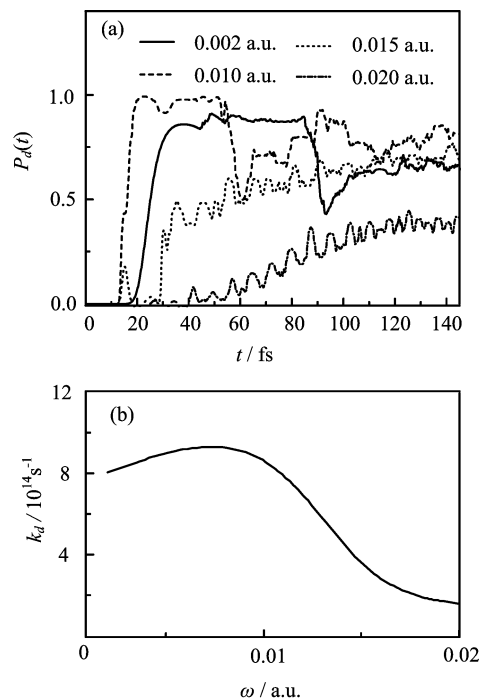


FIG. 2 (a) Variation of dissociation probability $P_d(t)$ with time in different field frequency (ω). (b) Dissociation rate constant k_d as a function of ω . Peak field-intensity $\varepsilon_0=0.08$ a.u. (2.91 PW/cm^2), temperature $T=0 \text{ K}$.

finding the system in a state that is not in the bound part of the spectrum of HBr^+ at a time t . It is seen that the dissociation probability in the early stage increases slowly and then is at a reasonable rate.

To understand profoundly the external field effect on dissociation phenomena, we compared dissociation probabilities $P_d(t)$ and dissociation rate constant k_d of the system (HBr^+) by perturbing with different field strength at zero temperature limit. The dissociation rate constant has been calculated by plotting $-\ln P_d(t)$ against t and computing the slope at time of raising the dissociation probability based on the following equation:

$$\frac{d[-\ln P_d(t)]}{dt} = k_d \quad (21)$$

We observed that with increase in field strength, the dissociation rate constant increases. We have studied the dissociation process against the frequency of the driving field when all the other parameters of the light remain constant. In Fig.2(a), we show $P_d(t)$ with time t for four different frequencies 0.002, 0.010, 0.015, and 0.020 a.u. of the used light field where the intensity of the light is fixed at 0.08 a.u. in each case. It is clear from the figure that by increasing frequency of the light field, $P_d(t)$ at a particular time increases up to certain frequency and then decreases. We have used four different frequencies 0.002, 0.010, 0.015, and 0.020 a.u. in our numerical experiment. The approximate resonance

energy from the ground to first excited state transition is 0.0118 a.u. From the figure, it is observed that $P_d(t)$ at a particular time increases when the frequency rises from 0.002 a.u. to 0.01 a.u. but gradually decreases when the frequency further rises from 0.01 a.u. to 0.02 a.u. through 0.015 a.u. Hence, it may be concluded that $P_d(t)$ at a particular time would be maximum when the frequency of the applied field is close to the resonance frequency of 0.018 a.u. In Fig.2(b) we have shown the corresponding frequency *vs.* dissociation rate constant. The figure shows that as the frequency of the used light increases the dissociation rate constant increases and passes through the maximum. The frequency at which the dissociation rate constant is maximum, matches more or less to the resonance frequency of the $0 \rightarrow 1$ transition. So it may conclude that if we fix the driving field frequency matching with the corresponding transition frequency the dissociation rate constant will be maximum and this is due to resonance activation. So the dissociation probability of the system will be less that the system will be stabilized beyond the $0 \rightarrow 1$ transition frequency which is reflected in the Fig.2 where the dissociation probability profile against time runs below for the higher frequency beyond the $0 \rightarrow 1$ transition frequency. This observation of stabilization at higher field frequency is in agreement with other theoretical studies on multiphoton process [39, 40].

To show the effect of temperature on the dissociation dynamics, we have gone through the wave packet [41, 42] formalism technique. We initially constructed a wave packet by the superposition of the different vibrational states with the initial coefficient governed by the Boltzmann distribution function (Eq.(8)). We have calculated k_d against temperature for continuous pulse which is shown in the Fig.3(a). It shows that with increase of temperature k_d increases. Figure 3(b) shows $P_d(t)$ for three different temperatures $T=200, 600,$ and 800 K. Here we have used continuous laser pulse with the pulse envelop function $S(t)=1$. It shows an increase of $P_d(t)$ with the increase of temperature. It may be due to increase in population at higher vibrational levels as temperature rises and hence facilitating escape from bound state. As a result, dissociation probability increases. We have shown $P_d(t)$ at different temperature for the other pulse shape functions in the Fig.3(c) which are of the same pattern.

The dependency of pulse envelop functions on k_d at non zero temperature has been shown for two types of pulses, one is the sinusoidal type and the other is the Gaussian type. Here t_p is connected to the pulse width by $\text{FWHM}=0.364 t_p$ for sinusoidal case and for Gaussian case it is $\sigma=4\ln 2(\text{FWHM})^{-2}$. In both the cases we have used the same pulse width. In Fig.4(a) we have shown the dependency of k_d on temperature. The pulse width is taken as 55 fs. Corresponding pulse duration (t_p) of the sinusoidal pulse would be $\text{FWHM}/0.364$ *i.e.* $55/0.364=151.1$ fs. The system will experience maximum field intensity when the pulse envelop function,

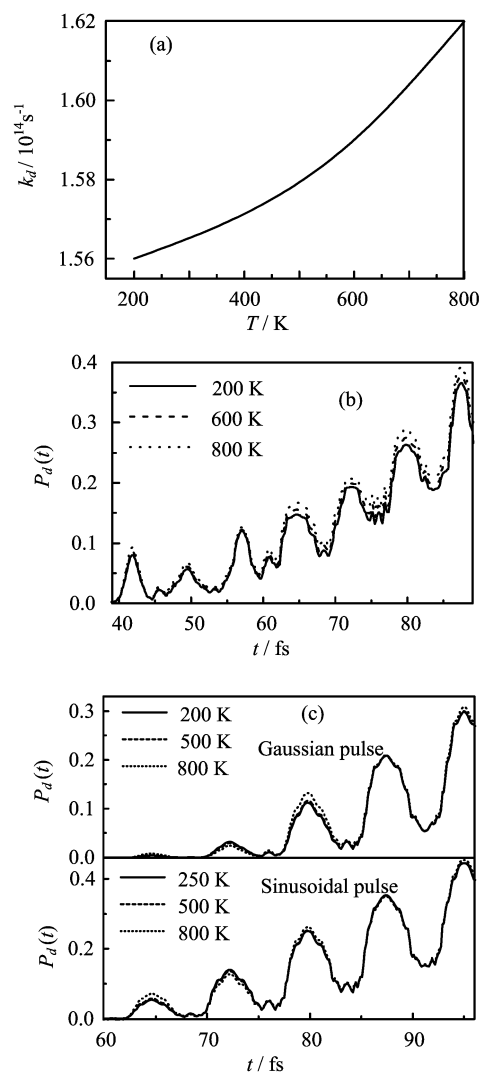


FIG. 3 (a) Dissociation rate constant (k_d) as a function of temperature. (b) The variation of dissociation probability ($P_d(t)$) with time at different temperatures. $\omega=0.02$ a.u. (4389 cm^{-1}) and $\varepsilon_0=0.08$ a.u. (2.91 PW/cm^2). (c) Variation of $P_d(t)$ with time at different temperatures in case of Sinusoidal (lower panel) and Gaussian (upper panel) shaped laser pulses. In both cases, $\text{FWHM}=55$ fs, $\omega=0.02$ a.u. (4389 cm^{-1}) and $\varepsilon_0=0.14$ a.u. (4.84 PW/cm^2).

$S(t)$ gets its maximum value *i.e.* for the sinusoidal pulse at $t=t_p/2$. The value is significant in the sense that it is the time around which $P_d(t)$ starts rising from zero value as observed in Fig.4(b). In Gaussian pulse, t_c is the time when field intensity goes to maxima. To make the comparison more realistic we set $t_c=t_p/2$ in Gaussian pulse. At that condition, it shows an increase of k_d with increase of temperature for both types of pulses, though the rise is not very high. The increase is non-linear type and rises more sharply at higher temperature. This is a common feature in both types of pulses, though the increase is comparatively more significant in Gaussian pulse. In general it is observed

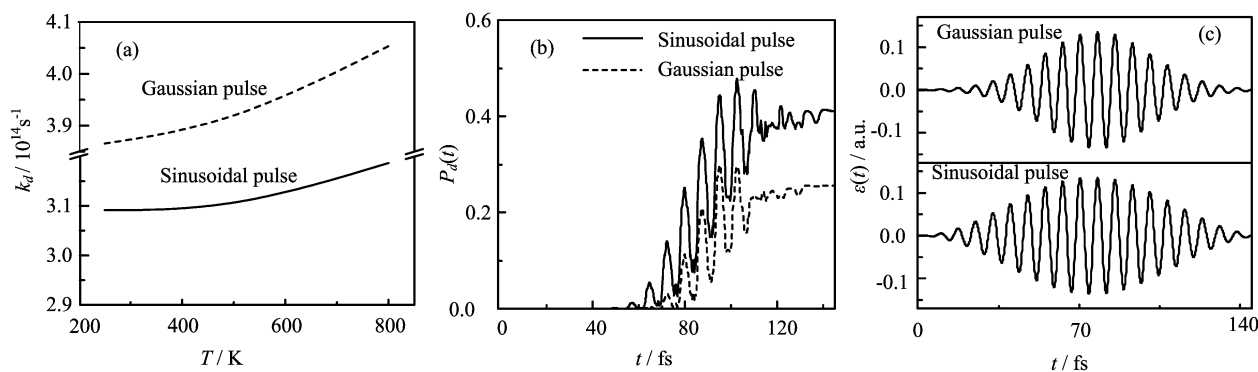


FIG. 4 (a) Dependence of k_d on temperature in case of Sinusoidal and Gaussian shaped laser pulses FWHM=55 fs, $\omega=0.02$ a.u. (4389 cm^{-1}), and $\varepsilon_0=0.14$ a.u. (4.84 PW/cm^2). (b) Variation of $P_d(t)$ with time for these two different types of laser field at 200 K, and (c) the laser field intensities variation with time t .

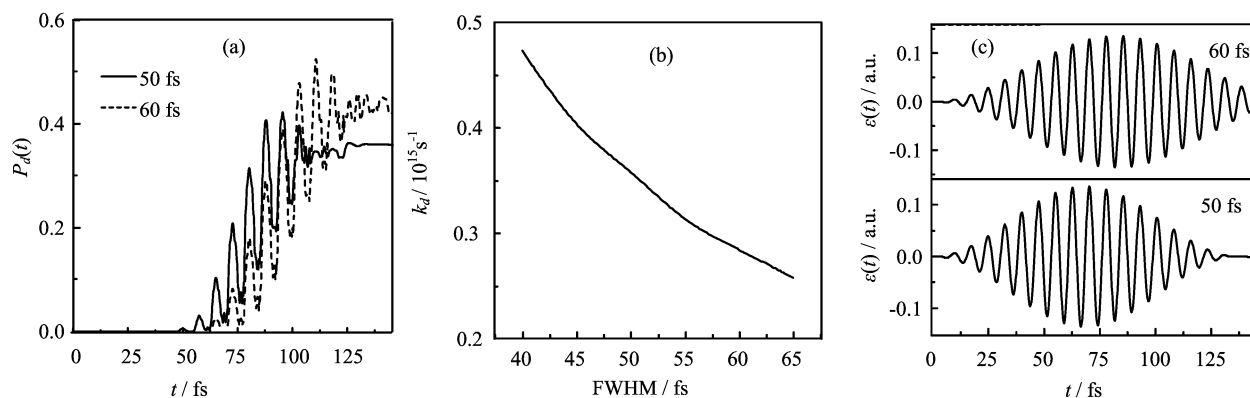


FIG. 5 (a) Variation of $P_d(t)$ with time t in case of sinusoidal laser pulse with two different FWHM values. (b) Dependence of k_d on FWHM. $\omega=0.02$ a.u. (4389 cm^{-1}) and $\varepsilon_0=0.14$ a.u. (4.84 PW/cm^2), $T=298\text{ K}$. (c) The field intensities variation with time t .

that the value of k_d in case of Gaussian pulse is quite higher than that of sinusoidal one. To explain it we have to look at Fig.4(c) where the comparison between the field intensities of these pulses shows a sharper increase in field intensity in case of the Gaussian pulse which should result in the rise of dissociation rate. However it is also noticed in Fig.4(c) that the sinusoidal pulse exerts more laser energy over a longer period of time. This should form more perturbation of the system and as a consequence we observe in Fig.4(b) that the dissociation probability reaches higher value over a longer period of time in case of the sinusoidal pulse.

To understand the effect of pulse in more details we choose sinusoidal pulse and vary its pulse width to show the effect of pulse width on k_d . The study was done using field of pulse width, FWHM varying from 45 fs to gradual increase up to 65 fs. In Fig.5(a) it shows $P_d(t)$ for FWHM of 50 fs and 60 fs only, and Fig.5(b) shows the dependency of k_d on FWHM from 45 fs to 65 fs. It is observed that k_d gradually decreases with increase in pulse width non-linearly. The decay rate gradually slows down at higher pulse width region that indicates k_d goes towards saturation. The field intensity of the

50 and 60 fs pulses is shown in Fig.5(c). It shows wider pulse create less sharp rise in the field intensity and thus one may expect lower dissociation rate of wider pulse which is observed in the figure. However, the lower panels show that the 60 fs pulse exerts comparatively more laser energy than that of 50 fs over a longer period of time. Due to greater perturbation, dissociation probability $P_d(t)$ reaches higher value over a longer period of time which is observed in Fig.5(a).

In bichromatic laser field one has the opportunity to control the dissociation through proper choice of the two frequencies. Figure 6 shows k_d as a function of frequencies ratio of two fields for fixed laser intensity 4.84 PW/cm^2 . Temperature is fixed as 298 K and pulse envelop function of the laser fields are of sinusoidal type. The interesting feature we observed is that k_d shows two peaks near the ratio $\omega_1/\omega_2=0.5$ and 1. When the two fields are commensurate with each other, they interfere constructively and thereby increasing the dissociation rate. Thus one can tune the dissociation rate by tuning the magnitude of the two frequencies.

To study the effect of phase difference between the

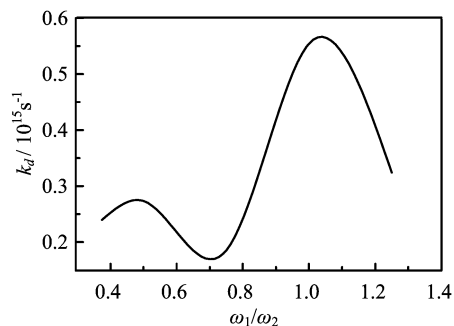


FIG. 6 Dependence of k_d on the frequency ratios ω_1/ω_2 of sinusoidal pulsed bichromatic lasers. ω_1 was fixed as 0.02 a.u. (4389 cm^{-1}) while ω_2 varied, $\varepsilon_0=0.14$ a.u. (4.84 PW/cm^2), FWHM=50 fs and $T=298$ K.

two electric fields, we may write

$$V'(x, t) = \varepsilon_0 S(t) \mu(x) \sin(\omega_1 t) + \varepsilon_0 S(t) \mu(x) \sin(\omega_2 t + \tau) \quad (22)$$

here τ is the relative phase between the bichromatic electric field components of photon energy $\hbar\omega_1$ and $\hbar\omega_2$. In Fig.7 we have plotted the dissociation rate constant as a function of the relative phase factor τ when all other parameters are fixed for both the field components. From Fig.7 it is seen that the dissociation rate constant decreases with the increase in the relative phase factor. As the value of τ increases the coherence between the two fields decreases and hence the dissociation rate constant decreases.

IV. CONCLUSION

We have tried to explore the thermal and pulse function effect on the photo-dissociation dynamics of diatomic molecular ion HBr⁺. We have calculated the dissociation probability and the dissociation rate constant of the ion concerned as a function of the various parameters of external electrical field and temperature. Our study reveals that with an increase of field intensity the dissociation probability of the ion increases and also the dissociation rate constant increases non-linearly up to a certain value. When the dissociation probability ($P_d(t)$) and dissociation rate constant (k_d) are studied as a function of frequency of the field, it passes through a maximum and the maximum occurs near a frequency of 0 \rightarrow 1 transition. Under the pulse shape variation of the used light field, it is observed that in case of Gaussian pulse the dissociation rate constant is slightly higher than that of sinusoidal pulse. It is expected as the field intensity rises sharply in case of Gaussian pulse and thus results in the rise of k_d . However, it is also noticed in the comparative studies that the sinusoidal pulse exerts more laser energy over a longer period of time. This should form more perturbation to the system and as a consequence, we observe that the disso-

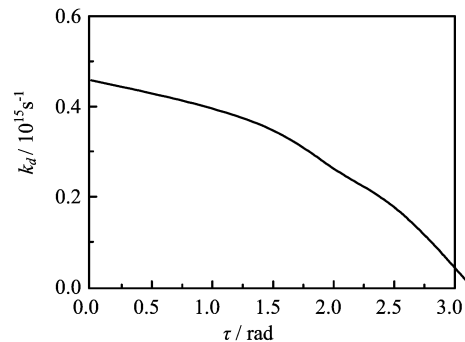


FIG. 7 Variation of k_d with the phase difference τ between two different electric field components of sinusoidal shaped bichromatic laser field. $\omega_1=\omega_2=0.02$ a.u. (4389 cm^{-1}), $\varepsilon_0=0.14$ a.u. (4.84 PW/cm^2), FWHM=50 fs, $T=298$ K.

ciation probability reaches higher value over a longer period of time in case of the sinusoidal pulse. In case of pulse width variation, it is observed that for higher pulse width the dissociation rate is slightly lower. We can expect this as wider pulse create slower rise in the field intensity and one may expect lower dissociation rate. But as the wider pulse exerts comparatively more laser energy over a longer period of time, so due to greater perturbation, the overall $P_d(t)$ reaches a higher value than the shorter one. In case of bichromatic field, the dissociation probability and the rates are relatively higher in case of commensurate frequencies than incommensurate one. The temperature has profound effect on the dissociation process and it is observed that the dissociation probability and rate increases non-linearly with temperature. We have also seen that the dissociation rate constant decreases with the increase in relative phase between the two bichromatic electric field components. We hope that our results on the dissociation dynamics of diatomic molecular ion will stimulate experimental work in this direction.

V. ACKNOWLEDGMENTS

The authors thank Dr. P. Sarkar from Visva-Bharati University for fruitful discussions. The authors also thank University Grants Commission, Government of India, for financial support through CAS program.

- [1] L. V. Keldysh, Sov. Phys. JETP. **20**, 1307 (1965).
- [2] A. M. Perelomov, V. S. Popov and M. V. Terent'ev, Sov. Phys. JETP. **23**, 924 (1966).
- [3] J. H. Posthumus, Rep. Prog. Phys. **67**, 623 (2004).
- [4] A. Giusti-Suzor, F. H. Mies, L. F. DiMauro, E. Charon, and B. Yang, J. Phys. B **28**, 309 (1995).
- [5] D. W. Lupo and M. Quack, Chem. Rev. **87**, 181 (1987).
- [6] F. Karlický, B. Lepetit, R. Kalus, and F. X. Gadéa, J. Chem. Phys. **134**, 084305 (2011).

- [7] H. Zhang, K. L. Han, Y. Zhao, G. Z. He, and N. Q. Lou, *Chem. Phys. Lett.* **271**, 204 (1997).
- [8] H. Zhang, K. L. Han, G. Z. He, and N. Q. Lou, *Chem. Phys. Lett.* **289**, 494 (1998).
- [9] J. Hu, K. L. Han, and G. Z. He, *Phys. Rev. Lett.* **95**, 123001 (2005).
- [10] K. Codling, L. J. Frasinski, and P. A. Hatherly, *J. Phys. B* **22**, L321 (1989).
- [11] K. Codling and L. J. Frasinski, *J. Phys. B* **26**, 783 (1993).
- [12] P. Dietrich and P. B. Corkum, *J. Chem. Phys.* **97**, 3187 (1992).
- [13] C. K. Mondal, *Int. J. Quantum Chem.* **103**, 258 (2005).
- [14] C. K. Mondal, *Int. J. Quantum Chem.* **108**, 15 (2008).
- [15] M. J. Davis and R. E. Wyatt, *Chem. Phys. Lett.* **86**, 235 (1982).
- [16] M. E. Goggin and P. W. Milonni, *Phys. Rev. A* **37**, 796 (1988).
- [17] A. D. Bandrauk and M. L. Sink, *J. Chem. Phys.* **74**, 1110 (1981).
- [18] S. Chelkowski, A. D. Bandrauk, and P. B. Corkum, *Phys. Rev. Lett.* **65**, 2355 (1990).
- [19] P. S. Dardi and S. K. Gray, *J. Chem. Phys.* **77**, 1345 (1982).
- [20] S. Chelkowski, A. D. Bandrauk, and P. B. Corkum, *Phys. Rev. Lett.* **65**, 2355 (1990).
- [21] S. Chelkowski and A. D. Bandrauk, *Phys. Rev. A* **41**, 6480 (1990).
- [22] S. Adhikari and S. P. Bhattacharyya, *Phys. Lett. A* **172**, 155 (1992).
- [23] G. Gangopadhyay and D. S. Ray, *J. Chem. Phys.* **97**, 4104 (1992).
- [24] R. C. Brown and R. E. Wyatt, *J. Chem. Phys.* **82**, 4777 (1985).
- [25] C. K. Mondal, P. Chaudhury, and S. P. Bhattacharyya, *Chem. Phys. Lett.* **311**, 400 (1999).
- [26] P. Lou, C. K. Mondal, S. Kang, K. Lee, K. K. Baek, and J. Y. Lee, *Chem. Phys.* **336**, 103 (2007).
- [27] S. Adhikari, P. Dutta, and S. P. Bhattacharyya, *Chem. Phys. Lett.* **199**, 574 (1992).
- [28] G. D. Purvis and R. J. Bartlett, *J. Chem. Phys.* **76**, 1910 (1982).
- [29] A. Debnarova, S. Techert, and S. Schmatz, *J. Chem. Phys.* **133**, 124309 (2010).
- [30] M. Mladenovic and S. Schmatz, *J. Chem. Phys.* **109**, 4456 (1998).
- [31] J. B. Foresman and M. J. Frish, *Exploring Chemistry with Electronic Structure Methods*, Pittsburgh, PA: Gaussian, Inc., (1996).
- [32] K. K. Baek and Y. Joo, *Chem. Phys. Lett.* **337**, 190 (2001).
- [33] K. P. Huber and B. Herzberg, *Molecular Spectra and Molecular Structure IV Constant of Diatomic Molecules*, New York: Van Nostrand, (1979).
- [34] J. Rafferty and W. G. Richards, *J. Phys. B* **6**, 1301 (1973).
- [35] C. C. Marston and G. G. B. Kurti, *J. Chem. Phys.* **91**, 3571 (1989).
- [36] G. G. Balint Kurti, C. L. Ward, and C. C. Marston, *Comput. Phys. Commun* **67**, 285 (1991).
- [37] U. V. Riss and H. D. Meyer, *J. Phys. B* **28**, 1475 (1995).
- [38] M. J. Haugh and K. D. Bayes, *J. Phys. Chem.* **75**, 1472 (1971).
- [39] M. Pont and M. Gravrila, *Phys. Rev. Lett.* **65**, 2362 (1990).
- [40] D. Richards, *J. Phys. B* **26**, 3223 (1993).
- [41] T. S. Chu, Y. Zhang, and K. L. Han, *Int. Rev. Phys. Chem.* **25**, 201 (2006).
- [42] T. S. Chu and K. L. Han, *Phys. Chem. Chem. Phys.* **10**, 2431 (2008).